The spatial density gradient of galactic cosmic rays and its solar cycle variation observed with the Global Muon Detector Network

M. Kozai[1], K. Munakata[1], C. Kato[1], S. Yasue[1], T. Kuwabara[2], J. W. Bieber[2], P. Evenson[2], M. Rockenbach[3], A. Dal Lago[4], N. J. Schuch[5], M. Tokumaru[6], M. L. Duldig[7], J. E. Humble[7], I. Sabbah[8], H. K. Al Jassar[9], M. M. Sharma[9], and J. Kota[10]

[1]Physics Department, Shinshu University, Matsumoto, Nagano 390-8621, Japan. [2]Bartol Research Institute and Department of Physics and Astronomy, University of Delaware, Newark, DE 19716, USA. [3]Universidade do Vale do Paraíba(UNIVAP), 12244-000, São José dos Campos, SP, Brazil. [4]National Institute for Space Research (INPE), 12227-010 São José dos Campos, SP, Brazil. [5]Southern Regional Space Research Center (CRS/INPE), P.O. Box 5021, 97110-970, Santa Maria, RS, Brazil. [6]Solar Terrestrial Environment Laboratory, Nagoya University, Nagoya, Aichi 464-8601, Japan. [7]School of Mathematics and Physics, University of Tasmania, Hobart, Tasmania 7001, Australia. [8]Department of Natural Sciences, College of Health Sciences, Public Authority of Applied Education and Training, Kuwait. [9]Physics Department, Kuwait University, Kuwait 13060. [10]Lunar and Planetary Laboratory, University of Arizona, Tucson, AZ 85721, USA.

Abstract. We analyze the long-term variation of the first order anisotropy observed with the Global Muon Detector Network (GMDN) on hourly basis and compare it with the diurnal and north-south anisotropies observed by a single muon detector at Nagoya in Japan. We confirmed that three components of the three dimensional (3D) anisotropy vector including the north-south component derived from two observations are fairly consistent with each other as long as the yearly mean value is concerned. From the 3D anisotropy vector corrected for the solar wind convection and the Compton-Getting effect arising from the Earth's orbital motion around the Sun, we deduce modulation parameters including the spatial density gradient and the parallel mean free path for the pitch angle scattering of GCRs in the turbulent interplanetary magnetic field (IMF). We find a close correlation between variations of the anisotropy parallel to the IMF with the solar wind speed. We also show the derived density gradient and mean free path varying with the solar activity- and magnetic-cycles. We discuss the physical implication of these variations by comparing with the prediction of the drift model.

Introduction

Based on the Parker's transport equation of GCRs in the heliosphere, We can deduce the large-scale spatial gradient of GCR density in the heliosphere from the observed directional anisotropy (or the streaming) of high energy GCR intensity. Only a global network of detectors can measure the dynamic variation of the anisotropy accurately and separately from the temporal variation of the GCR density (or the isotropic intensity). The GMDN started measuring the **three dimensional (3D) anisotropy on hourly basis** with two hemisphere observations using a pair of muon detectors at Nagoya (Japan) and Hobart (Australia) in 1992. The current network consisting of four muon detectors in Nagoya, Hobart, Sáo Martinho (Brazil) and Kuwait University (Kuwait) was completed in 2006.

The solar cycle variation of the modulation parameters alters the global distribution of GCR density and causes long-term variations of the anisotropy at the Earth [1]. [2] analyzed the GCR anisotropy and observed with a single multidirectional muon detector at Nagoya in Japan and reported the component anisotropy parallel to the IMF changing with a significant **correlation with the solar wind velocity** on a yearly mean basis. Analyses of the diurnal variation observed with a single detector, however, can give correct anisotropy only when the anisotropy is stationary at least over one day. Also the correlation with the solar wind velocity should be analyzed with better time resolution, since both the anisotropy and solar wind velocity often show dynamic variations within one day ([3] [4]). In this paper, **we analyze the long-term variation of the anisotropy observed with the GMDN over 21 years between 1992 and 2012**.

Data analysis and results

We analyze the pressure corrected hourly count rate $I_{i,j}(t)$ of muons recorded by the *j*-th directional channel of the *i*-th detector in the GMDN at the universal time *t* and derive three components ($\xi_x^{\rm GEO}$, $\xi_y^{\rm GEO}$, $\xi_z^{\rm GEO}$) of the first order anisotropy in the geographic (GEO) coordinate system by best-fitting the following model function to $I_{i,j}(t)$.

$$I_{i,j}^{fit}(t) = I_{i,j}^{0}(t) + \xi_x^{\rm GEO}(t)\left(c_{1i,j}^{1}\cos\omega t_i - s_{1i,j}^{1}\sin\omega t_i\right) + \xi_y^{\rm GEO}(t)\left(s_{1i,j}^{1}\cos\omega t_i + c_{1i,j}^{1}\sin\omega t_i\right) + \xi_z^{\rm GEO}(t)c_{1i,j}^{0}$$

where $I_{i,j}^{0}(t)$ is a parameter representing the contributions from the omnidirectional intensity and the atmospheric temperature effect, t_i is the local time in hour at the *i*-th detector, $c_{1i,j}^{1}$, $s_{1i,j}^{1}$ and $c_{1i,j}^{0}$ are the so-called coupling coefficients and $\omega = \pi/12$. The coupling coefficients are calculated by using the response function of atmospheric muons to the primary cosmic rays ([5] [6]) and by assuming the rigidity independent anisotropy with the upper limiting rigidity set at 10^5GV far above the maximum rigidity of the response.

In deriving the anisotropy vector $\boldsymbol{\xi}$, we also apply an analysis method developed for removing the atmospheric temperature effect from the derived anisotropy (see [7]). The deduced anisotropy is averaged in each period of the toward and away IMF sectors identified from the hourly IMF data in the omnitape [8] in every Carrington Rotation (CR). The yearly mean anisotropy is then calculated by averaging $\boldsymbol{\xi}$s in toward and away sectors in each year.

For comparison, we also derive the anisotropy from the observation by a single multidirectional muon detector at Nagoya (hereafter Nagoya) which is a component detector of GMDN. We deduce the equatorial component of $\boldsymbol{\xi}$ from the mean diurnal variation of the hourly counting rate in each IMF sector in every CR, while we derive the north-south (NS) component $\xi_z^{\rm GEO}$ from the daily mean GG-component, which is a difference combination between intensities recorded in the north- and south-viewing channels and has long been used as a good measure of the NS anisotropy [9]. Figures 1 compares yearly averages of $\boldsymbol{\xi}$ derived from two analyses of the GMDN and Nagoya data. It is clear that **the temporal variations by GMDN and Nagoya are consistent with each other, confirming that the analysis of the single muon detector data gives reliable 3D anisotropy as long as the yearly mean anisotropy is concerned [2].**

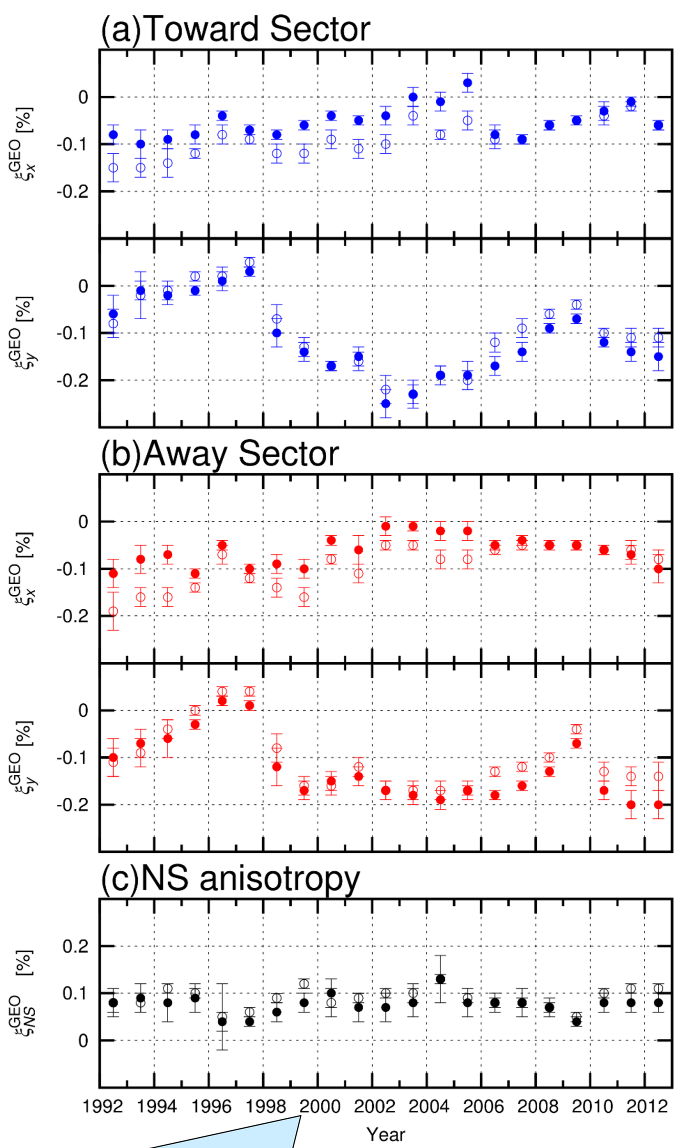

Figure 1: Temporal variations of anisotropies obtained by GMDN and Nagoya in GEO coordinate system. The solid (open) circles represent the anisotropy by GMDN (Nagoya). (a) and (b): *x* and *y* components in the toward and away sector. (c): the NS anisotropy $\xi_{NS}^{\rm GEO}$ which is the difference $((\xi_z^T - \xi_z^A)/2)$ between mean $\xi_z^{\rm GEO}$s in the toward (ξ_z^T) and away (ξ_z^A) sectors.

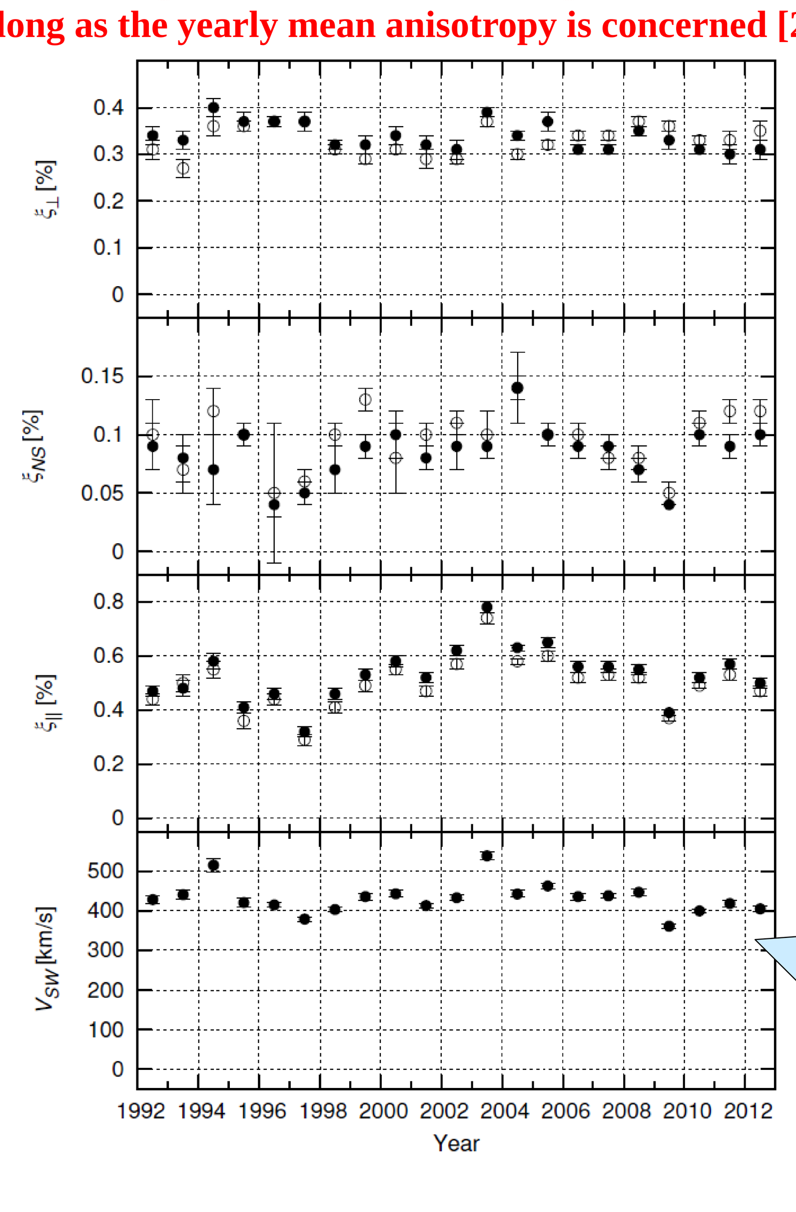

Figure 2: Temporal variations of parallel, perpendicular and north-south components of the anisotropy and solar wind speed V_{SW}. The solid (open) circles represent the anisotropy by GMDN (Nagoya).

The anisotropies obtained by GMDN and Nagoya in each IMF sector are transformed to the geocentric solar ecliptic (GSE) coordinate system. We then correct the anisotropy for the solar wind convection anisotropy using the solar wind velocity from the omnitape data averaged in each sector and for the Compton-Getting anisotropy arising from the Earth's 30 km/s orbital motion around the Sun and obtain the component anisotropies parallel ($\xi_{||}$) and perpendicular ($\xi_{\perp}$) to the IMF in the ecliptic plane. Figure 2 shows the temporal variations of the $\xi_{||}$, $\xi_{\perp}$, ξ_{NS} and solar wind speed V_{SW}. **We find a clear positive correlation between $\xi_{||}$ and V_{SW} as reported in [2]. $\xi_{||}$ also shows a 22-year variation with slightly larger value at the solar minimum in A < 0 (2001-2012) than A > 0 (1992-1999) solar polarity as reported by [1], while no 22-year variation is seen in V_{SW}.** ξ_{NS}, on the other hand, varies with 11-year cycle, while $\xi_{\perp}$ shows no solar cycle variation.

Following the analyses by [1], we deduce the modulation parameters, the bidirectional latitudinal gradient $G_{|z|}$, the radial density gradient G_r and the mean free path (m.f.p.) of the pitch angle scattering parallel to the IMF, $\lambda_{||}$ from $\xi_{||}$, $\xi_{\perp}$ and ξ_{NS}. For this calculation, we assume that the ratio of the perpendicular m.f.p. ($\lambda_{\perp}$) to the parallel m.f.p ($\lambda_{||}$) is 0.05 and constant as adopted by [7]. Figure 3 displays temporal variations of modulation parameters obtained by GMDN and Nagoya muon detector. The following 22-year and 11-year cycle variations are clearly seen. **First, $G_{|z|}$ is positive in A > 0 epoch indicating the local minimum of the density on the Heliospheric Current Sheet (HCS), while it is negative in A < 0 epoch indicating the local maximum on the HCS as predicted by the drift model. Second, a significant 11-year variations are seen in G_r and $\lambda_{||}$ with a clear positive and negative correlations with the IMF magnitude, respectively.**

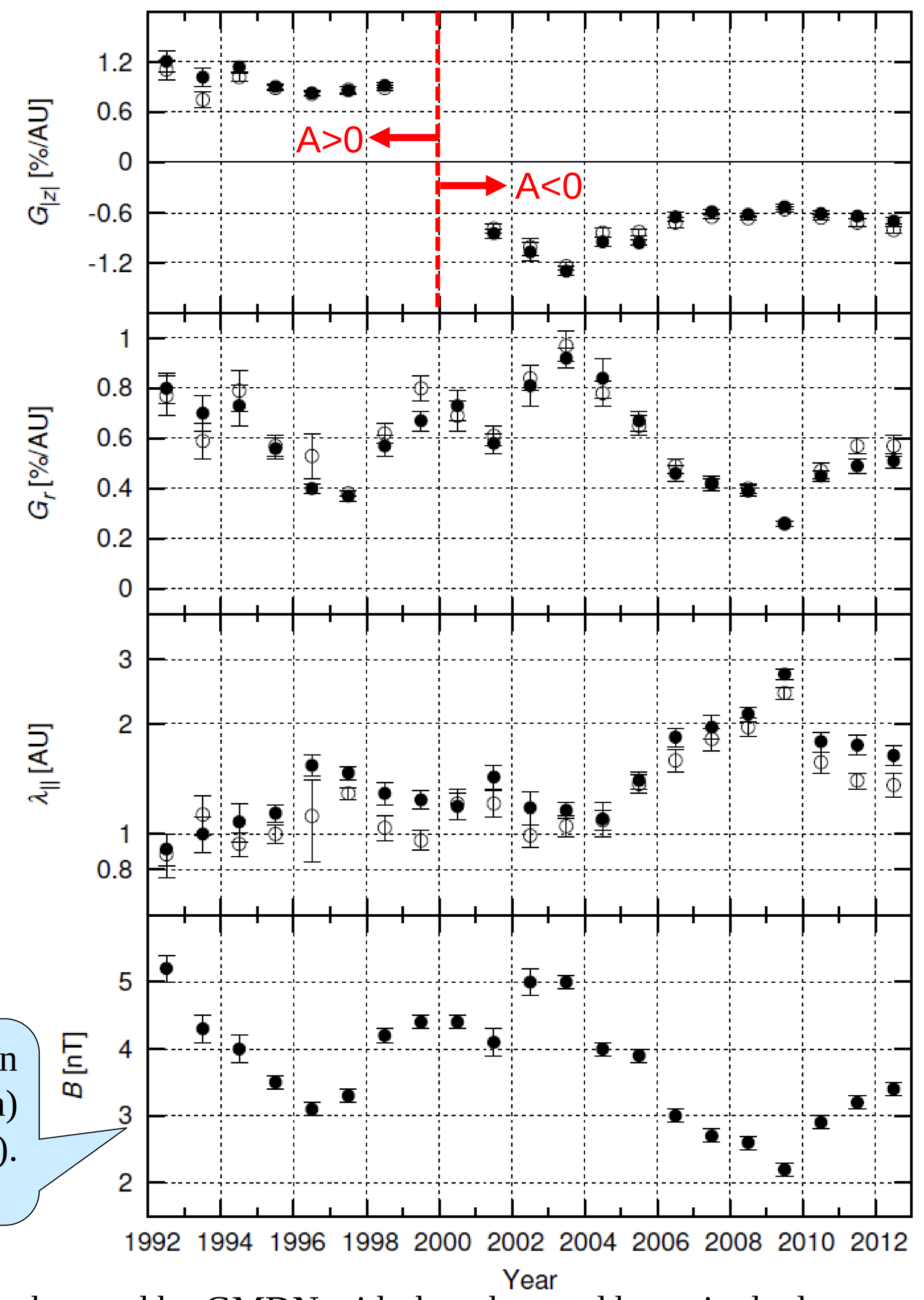

Figure 3: Temporal variations of modulation parameters and the IMF magnitude. The solid (open) circles represent the parameter by GMDN (Nagoya). Note that the vertical axis of $\lambda_{||}$ is logarithmic.

Summary

We compared the 3D anisotropy of GCR intensity observed by GMDN with that observed by a single detector at Nagoya in 1992-2012. Our analysis of the GMDN data gives the anisotropy on hourly basis with **better time resolution than the traditional analyses of the diurnal variation of cosmic ray intensity observed by a single multidirectional detector** such as Nagoya. We confirmed that the 3D anisotropy and the modulation parameters derived from two analyses are **fairly consistent** with each other as long as the yearly mean value is concerned. Particularly, the NS anisotropies derived from two analyses are quite consistent proving the reliability of these analyses.

It is found that $G_{|z|}$ is positive in A > 0 epoch indicating the local minimum of the GCR density on the Heliospheric Current Sheet, while it is negative in A < 0 epoch indicating the local maximum on the HCS, **in accord with the drift model prediction**. A significant **11-year variations are seen in $\boldsymbol{G_r}$ and $\boldsymbol{\lambda_{||}}$** with a clear positive and negative correlations with the IMF magnitude *B*, respectively. The observed **$\boldsymbol{\xi_{||}}$ shows a 22-year variation** with slightly larger value at the solar minimum in A < 0 epoch (2001-2012) than in A > 0 epoch (1992-1998) as reported by [1]. This variation of $\xi_{||}$ is responsible to the well known 22-year variation of the phase of the diurnal variation [10]. We also found a clear correlation of $\boldsymbol{\xi_{||}}$ with the solar wind velocity V_{SW} wich shows no clear variation.

Discussion: 22-year variations of the modulation parameters

Figure 4 shows the correlations between G_r and $\lambda_{||}$ and between $\xi_{||}$ and V_{SW}, while table 1 summarizes correlation and regression coefficients of each correlation. Modulation parameters and $\xi_{||}$ in this figure are all derived from the analyses of the GMDN data. It is seen in figure 4(a) and table 1(1) that the regression lines in A > 0 and A < 0 epochs are almost parallel to each other, with the line in A < 0 shifted upward (or to the right) indicating larger G_r (or $\lambda_{||}$) in A < 0 epoch. Note that the larger G_r in A < 0 epoch is consistent with the drift model prediction [11].

It is also noted that there is a clear positive correlation between $\xi_{||}$ and V_{SW} as shown in figure 4(b). The vertical difference between $\xi_{||}$s in A > 0 and A < 0 epochs for the same value of V_{SW} is only about 0.1 %, while $\xi_{||}$ varies for about 0.2 % in association with 100 km/s variation in V_{SW} according to the regression coefficients in table 1(2). This implies that **the contribution from the V_{SW} effect should be removed for accurately analyzing the 22-year variation of $\xi_{||}$**. We derive the $\xi_{||}$ corrected for the solar wind variation by normalizing V_{SW} to 450km/s on yearly basis along the regression line $f(V_{SW}) = aV_{SW} + b\ (a, b = const.)$ in A > 0 or A < 0 epoch displayed in Figure 4(b). Figure 5 shows the corrected $\xi_{||}$ and the uncorrected $\xi_{||}$. **The corrected $\xi_{||}$ is roughly constant in each solar polarity and shows a 22-year variation** more clearly than in figure 2. The average value of $\xi_{||}$ is 0.49±0.02% (0.61±0.02%) in A > 0 (A < 0) epoch.

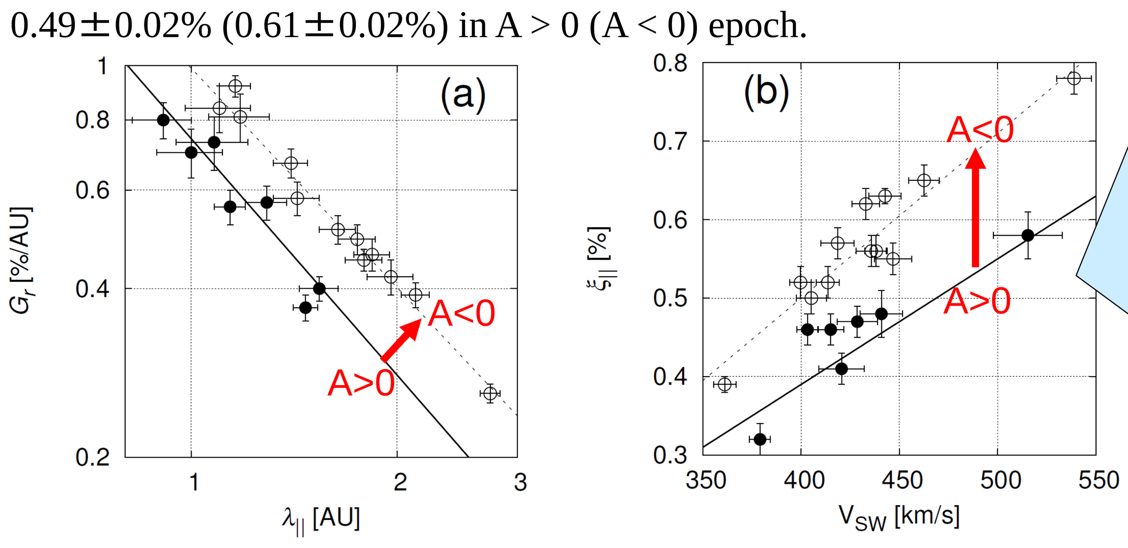

Figure 4: (a)Scatter plot between $\lambda_{||}$ and G_r in figure 3. (b)Scatter plot between V_{SW} and $\xi_{||}$ in figure 2. In each panel, the solid circles with the solid regression line represent the yearly mean values in A > 0 solar polarity epoch (1992-1998) while the open circles with the dotted regression line represent yearly mean values in A < 0 (2001-2012). Years (1999 and 2000) when the polarity reversal was ongoing are excluded from this plot. Note thea horizontal and vertical axes of panel (a) are in logarithmic scale.

	x axis	y axis	A	r	a
(1)	$\ln\lambda_{\|\|}$ [ln(AU)]	$\ln G_r$ [ln(%/AU)]	+	-0.95	-1.4±0.3
			−	-0.99	-1.3±0.1
(2)	V_{SW} [100km/s]	$\xi_{\|\|}$ [%]	+	0.90	0.16±0.04
			−	0.95	0.21±0.03

Table 1: The correlation coefficient r and the regression coefficient a between the yearly mean values on x and y axes in figure 4 for each of A > 0 and A < 0 epochs.

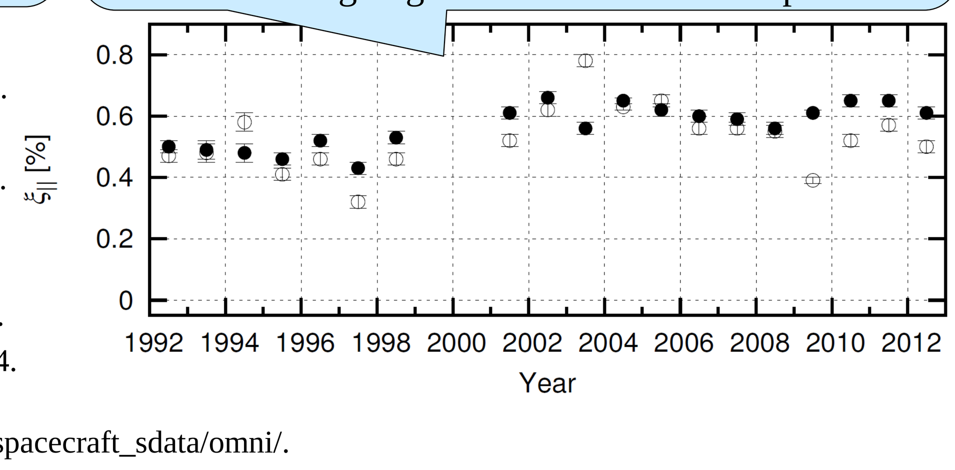

Figure 5: Temporal variations of $\xi_{||}$ corrected (solid circles) and uncorrected (open circles) for the variation of V_{SW}. Years (1999 and 2000) when the polarity reversal was ongoing are excluded from this plot.

REFERENCES

[1] J. Chen and J. W. Bieber, Astrophys. J. **405** (1993) 375-389.
[2] K. Munakata et al., Proc. 33rd International Cosmic Ray Conference in Rio de Janeiro (2013) paper ID:0039.
[3] Kuwabara et al., J. Geophys. Res. **114** (2009) A05109.
[4] Fushishita et al., Astrophys. J. **715** (2010) 1239-1247.
[5] K. Murakami et al., IL Nuovo Cimento **2C** (1979) 635-651.
[6] C. Baker et al., J. Geomag. Geoelectr. **42** (1990), 1137-1144.
[7] Y. Okazaki et al., Astrophys. J. **681** (2008) 693-707.
[8] omnitape-data are available at ftp://nssdcftp.gsfc.nasa.gov/spacecraft_data/omni/.
[9] M. Laurenza et al., J. Geophys. Res. **108** (2003) 1069-1075.
[10] T. Thambyahpillai and H. Elliot, Nature **171** (1953) 918-920.
[11] J. Kota and J. R. Jokipii, Astrophys. J. **265** (1983) 573-581.